Direct numerical simulation of a turbulent wake: the non-equilibrium dissipation law

T. Dairay[a,*], J.C. Vassilicos[a]

[a]*Department of Aeronautics, Imperial College London, London SW7 2AZ, United Kingdom*

Abstract

A Direct Numerical Simulation (DNS) study of an axisymmetric turbulent wake generated by a square plate placed normal to the incoming flow is presented. It is shown that the new axisymmetric turbulent wake scalings obtained recently for a fractal-like wake generator (Dairay et al., 2015), specifically a plate with irregular multiscale periphery placed normal to the incoming flow, are also present in an axisymmetric turbulent wake generated by a regular square plate. These new scalings are therefore not caused by the multiscale nature of the wake generator but have more general validity.

Keywords: Direct numerical simulation, Turbulence, Wakes

1. Introduction

Axisymmetric turbulent wakes have been extensively studied experimentally and numerically (see for example Johansson et al., 2003). A problem of particular interest remains however the prediction of the scaling laws for the wake's width δ and the centreline velocity deficit u_0 along the streamwise distance x. For the

*phone: +334-72-18-61-57

Email addresses: tdairay@hotmail.fr (T. Dairay), j.c.vassilicos@imperial.ac.uk (J.C. Vassilicos)

turbulent axisymmetric and self-preserving wake, these scalings laws can be derived from knowledge of the dissipation rate ε scalings (Townsend, 1976; George, 1989). In a recent study, Nedić et al. (2013) proposed an extension of the theory established in George (1989) assuming the non-equilibrium dissipation scaling (see Vassilicos, 2015, for details)

$$\varepsilon = C_\varepsilon \frac{K^{3/2}}{\delta} \quad \text{with } C_\varepsilon \sim Re_G^m / Re_l^m \tag{1}$$

where K is the turbulent kinetic energy, Re_G is a global Reynolds number determined by the inlet conditions and Re_l is a local Reynolds number based on local velocity and length scales. This theory has recently been tested in detail and revised by Dairay et al. (2015). Invoking an assumption of constant anisotropy, Dairay et al. (2015) have shown that it is possible to derive scaling laws for u_0 and δ for any values of the exponent m in (1) (this assumption actually replaces the usual assumption of self-similarity of every single term of the turbulent kinetic energy equation which turns out to be incorrect for some of the terms). They obtain $\delta(x)/\theta = B\left((x-x_0)/\theta\right)^\beta$ and, $u_0(x)/U_\infty = A\left((x-x_0)/\theta\right)^\alpha$ where θ is the momentum thickness, U_∞ is the freestream velocity, x_0 is a virtual origin, $\beta = (1+m)/(3+m)$, $\alpha = -2\beta = -2(1+m)/(3+m)$, $B \sim (L_b/\theta)^{\frac{2m}{3+m}}$ and $A = B^{-2}$. In Dairay et al. (2015), these predictions have been found to be in agreement with both numerical and experimental data for an axisymmetric turbulent wake generated by an irregular plate. The aim of this paper is to use DNS data to interrogate the existence of the new non-equilibrium dissipation law (1) and its wake-law consequences in a more "conventional" turbulent wake generated by a square plate.

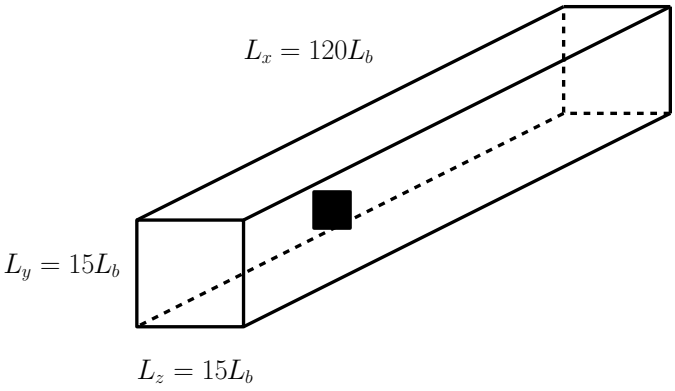

Figure 1: Schematic view of the computational domain.

2. Flow configuration and numerical methods

In the present study, a turbulent wake is generated by a square plate of surface area A placed normal to the incoming flow (see figure 1 for illustration). The surface area of the square plate is the same as the one of the irregular plate used in Dairay et al. (2015). In the Cartesian coordinate system $(O;x,y,z)$, the domain is $\Omega = [-x_p, L_x - x_p] \times [-L_y/2, L_y/2] \times [-L_z/2, L_z/2]$ where $x_p = 10L_b$ is the longitudinal location of the plate, the origin O is located at the centre of the plate and $L_x \times L_y \times L_z = 120L_b \times 15L_b \times 15L_b$ where $L_b = \sqrt{A}$ is the reference length of the flow (see figure 1). For the sake of simplicity the radial distance $r = \sqrt{y^2 + z^2}$ and the polar angle $\varphi = \arctan(y/z)$ are also introduced hereinafter. Mean quantities $\langle f \rangle (x,r)$ of a field $f(x,r,\varphi,t)$ are estimated by averaging over time and over the homogeneous polar direction φ in the cylindrical coordinate system (x,r,φ). The mean streamwise velocity component $\langle u_x \rangle (x,r)$ is denoted U. The momentum thickness θ is defined by $\theta^2 = (1/U_\infty^2) \int_0^\infty U_\infty (U_\infty - U)\, r dr = const.$

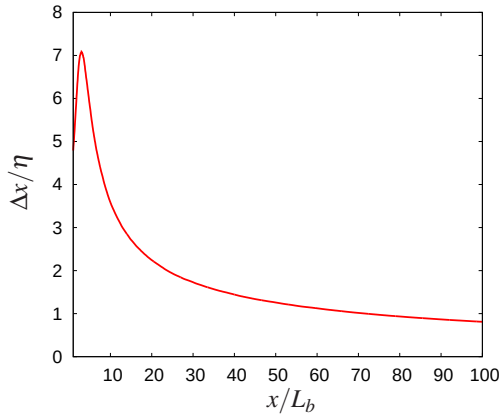

Figure 2: Streamwise evolution of the ratio $\Delta x/\eta$. The Kolmogorov microscale η has been computed on the basis of the maximum value of $\varepsilon(x,r)$ along r.

and the wake's width is here characterised by the integral wake's width δ, with $\delta^2(x) = (1/u_0)\int_0^\infty (U_\infty - U)\, rdr$ where $u_0(x) = U_\infty - U(x, r/L_b = 0)$ is the centreline velocity deficit. The global Reynolds number Re_G based on the reference length L_b and the freestream velocity U_∞ is $Re_G = 5000$. The local Reynolds number Re_l is defined by $Re_l(x) = \sqrt{K_0(x)}\delta(x)/\nu$ where K_0 is the turbulent kinetic energy at a centreline location.

The finite difference code *Incompact3d* (Laizet and Lamballais, 2009; Laizet et al., 2010) is used to solve the incompressible Navier-Stokes equations. The modelling of the plate is performed by an Immersed Boundary Method, following a procedure proposed by Parnaudeau et al. (2008). Inflow/outflow boundary conditions are assumed in the streamwise direction with a uniform fluid velocity U_∞ without turbulence as inflow condition and a 1D convection equation as outflow condition. The boundary conditions in the two spanwise directions are periodic. The computational domain is discretized on a Cartesian grid of $n_x \times n_y \times n_z = 3841 \times 480 \times 480$ points. In terms of Kolmogorov microscale η, as

illustrated in figure 2, the spatial resolution is at worst $\Delta x = \Delta y = \Delta z \approx 7\eta$ (where the turbulence is at its most intense) and at best $\Delta x = \Delta y = \Delta z \approx 0.8\eta$ (at the end of the computational domain where the turbulence has decayed). In the range $10 \leq x/L_b \leq 100$, which is the range of interest of our study, the spatial resolution is always below 4η. In a recent resolution study, Laizet et al. (2015) have shown that a spatial resolution of 7η or 5η is sufficient to reproduce experimental results with an error margin of about 10% or 5% respectively (for one-point first and second order statistics). They also showed that quantities such as the turbulence dissipation rate require a resolution of at least 4η to be well captured. For the spatial derivatives, sixth-order centred compact schemes (Lele, 1992) are used. To control the residual aliasing errors, a small amount of numerical dissipation is introduced only at scales very close to the grid cutoff. This very targeted regularization is ensured by the differentiation of the viscous term that is sixth-order accurate (Lamballais et al., 2011). The time integration is performed using an explicit third-order Adams-Bashforth scheme with a time step $\Delta t = 5 \times 10^{-3} L_b/U_\infty$ (corresponding to a CFL number of 0.16 and ensuring $\Delta t < 0.014\tau_\eta$ where τ_η is the Kolmogorov time-scale). Full details about the code "Incompact3d" can be found in Laizet and Lamballais (2009); Laizet et al. (2010); Laizet and Li (2011) (see also the link `www.incompact3d.com`).

The collection of data for the turbulent statistics is done over a time $T = 3850 L_b/U_\infty$, corresponding to approximately 25 seconds of the experiments in Nedić et al. (2013) and to 423 cycles based on the Strouhal number $St = f_{vs} L_b/U_\infty = 0.11$ associated with the vortex shedding frequency f_{vs} (see Nedić et al., 2013). This time is also the same as the one used in Dairay et al. (2015) ensuring good convergence of the DNS statistics.

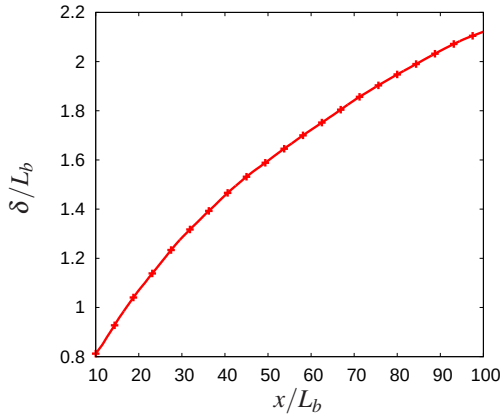

Figure 3: Streamwise evolution of the wake width δ/L_b.

The streamwise evolution of δ is plotted in figure 3. At $x = 100L_b$ (the most distant streamwise location that we are considering in the present paper), $\delta \approx 2.12L_b$. This means that the domain half-width is $L_y/2 = L_z/2 = 7.5L_b \approx 3.54\delta$ at $x = 100L_b$. According to Redford et al. (2012), the critical value needed to ensure that the lateral boundary conditions do not affect the wake development is $L_z/2 = L_y/2 \approx 2.95\delta$. The lateral dimensions of our domain therefore appear sufficiently large to avoid any significant contamination from the lateral boundaries even at $x = 100L_b$.

The DNS data can first be used to assess the validity of the local isotropy assumption commonly used in the experimental framework. In figure 4 we compare $\varepsilon_{iso} = 15\nu \left\langle (\partial u'_x/\partial x)^2 \right\rangle$ with the actual dissipation rate $\varepsilon_{full} = 2\nu \left\langle s_{ij} s_{ij} \right\rangle$ where $s_{ij} = (1/2)\left(\partial u'_i/\partial x_j + \partial u'_j/\partial x_i\right)$. It is clear from figure 4 (right) that $\varepsilon_{iso}/\varepsilon_{full}$ lies between 0.96 and 1.04 in the range $10 \leq x/L_b \leq 100$.

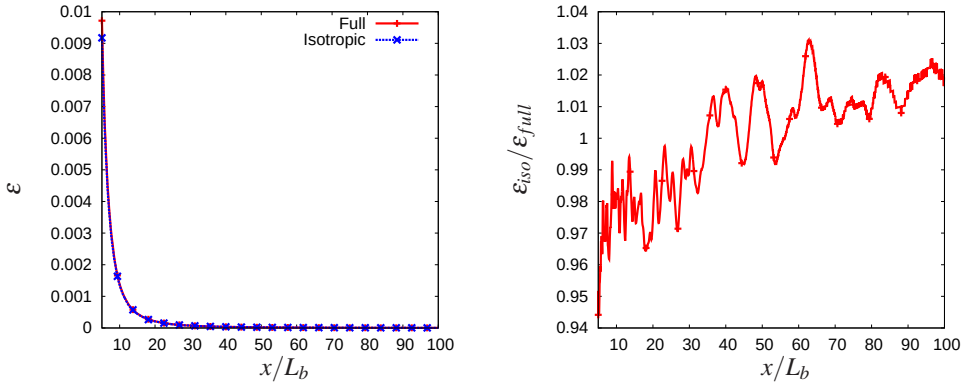

Figure 4: Centreline evolution of the full and isotropic dissipation (left) and of the ratio $\varepsilon_{iso}/\varepsilon_{full}$ (right).

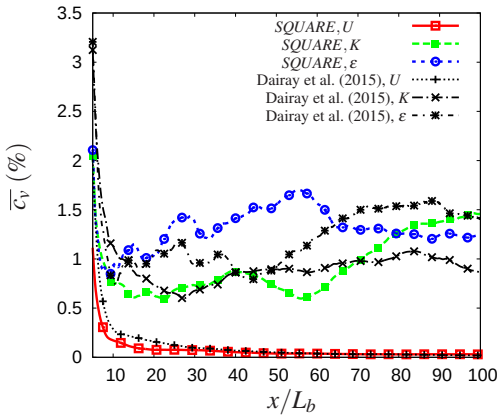

Figure 5: Streamwise evolution of the radially averaged coefficient of variance $\overline{c_v}$ for the mean velocity, turbulent kinetic energy and the dissipation profiles for the square plate case compared to the irregular plate data of Dairay et al. (2015).

3. Axisymmetry of wake statistics

A quantitative evaluation of the statistical axisymmetry of the flow generated by the square plate can been obtained by computing the mean values of the coefficient of variance $c_v(x,r) \equiv 100\sqrt{\left(1/N_\varphi\right)\sum_\varphi \left(S(x,r,\varphi) - \langle S\rangle(x,r)\right)^2}/\langle S\rangle(x,r)$ where N_φ is the number of polar angles and S stands for mean flow, turbulent kinetic energy or dissipation rate of turbulent kinetic energy. The streamwise variations of the radially averaged coefficient of variance $\overline{c_v}(x) \equiv (1/N_r)\sum_r c_v(x,r)$ are plotted in figure 5 while the irregular plate data of Dairay et al. (2015) are added for comparison. Figure 5 shows that, at $x = 10L_b$, there is already less than 4% variation in all statistics demonstrating the good axisymmetry of the flow generated by the square plate at $x > 10L_b$.

4. Similarity of the axisymmetric turbulent wakes

The axisymmetry of the flow generated by the square plate has been carefully checked. The next step of the analysis is to investigate the similarity properties of mean flow statistics. Self-similar forms are considered for the mean velocity, Reynolds shear-stress, turbulent kinetic energy and dissipation profiles as follows: $U_\infty - U(x,r) = u_0(x)f(r/\delta)$, $R_{xr}(x,r) = \langle u'_x u'_r\rangle(x,r) = R_0(x)g_{12}(r/\delta)$, $K(x,r) = K_0(x)h(r/\delta)$ and $\varepsilon(x,r) = D_0(x)e(r/\delta)$ where $f(0) = 1$. Streamwise mean velocity U profiles scaled by the centreline velocity deficit u_0 and the wake width δ are plotted in figure 6 for different streamwise distances. In the same way as for the irregular plate case in Dairay et al. (2015), these profiles are clearly self-similar for $x \geq 10L_b$. Reynolds shear stress $\langle u'_x u'_r\rangle$, turbulent kinetic energy K and dissipation rate ε profiles are respectively plotted in figures 7 (left), 8 (top left) and 9 with R_0, K_0 and D_0 set to be the maximum values along r of $\langle u'_x u'_r\rangle(x,r)$,

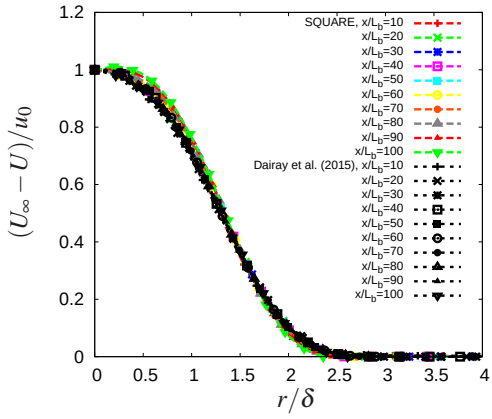

Figure 6: Mean flow profiles at different streamwise distances plotted using similarity scalings. The data of Dairay et al. (2015) are added for comparison.

$K(x,r)$ and $\varepsilon(x,r)$. These figures strongly suggest that these three quantities are self-similar in the region $x/L_b \geq 20$.

In addition, figure 7 (right) shows that the DNS data support the prediction of George (1989) that $R_0 \sim U_\infty u_0 \frac{d}{dx}\delta$ at least in the region $x/L_b \geq 20$. However, in agreement with Dairay et al. (2015), the square plate data do not endorse the scaling $K_0 \sim u_0^2$ predicted by George (1989) and Townsend (1976) as can be seen in figure 8 (top right).

In fact, K_0 scales in the same way as R_0 in the region $x/L_b \geq 20$ (see figure 8 (bottom centre)) in agreement with the assumption of constant anisotropy introduced by Dairay et al. (2015) for an axisymmetric wake generated by an irregular plate. In a very different context, Pantano and Sarkar (2002) have also observed a constant anisotropy with respect to the Mach number value in compressible shear layers (they did not study the anisotropy of the Reynolds stress along $r = \delta(x)$ as in the present study but they compared the peak turbulent intensities in different experiments and DNS). For the square plate case considered in this study, even

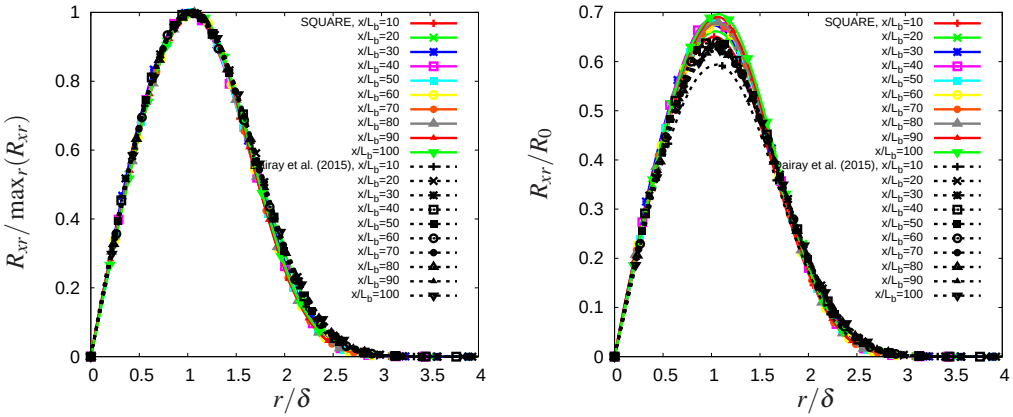

Figure 7: Reynolds shear stress profiles at different streamwise distances plotted using similarity scalings with $R_0 = \max_r R_{xr}$ (left) and $R_0 \sim u_0 U_\infty (d\delta/dx)$ (right). The data of Dairay et al. (2015) are added for comparison.

if the ratio of the r.m.s. of u'_x to the r.m.s. of u'_r along $r = \delta(x)$ plotted in figure 10 (left) is slightly increasing with streamwise distance, the fact that K_0 scales in the same way as R_0 and not with u_0^2 is confirmed when comparing the streamwise evolutions of both K_0/R_0 and K_0/u_0^2 in figure 10 (right).

In the following section we investigate the scalings and streamwise evolution of the dissipation rate focusing only on the square plate case considered in this study.

5. Streamwise evolution of the dissipation, wake width and velocity deficit scalings

Figure 11 shows that $C_\varepsilon = \varepsilon\delta/K^{3/2}$ grows with streamwise distance x both on and off the centreline, in clear disagreement with the equilibrium law $C_\varepsilon = const$ (corresponding to $m = 0$ in equation (1)). This observation is consistent with the findings of Dairay et al. (2015) concerning turbulent wakes generated by an

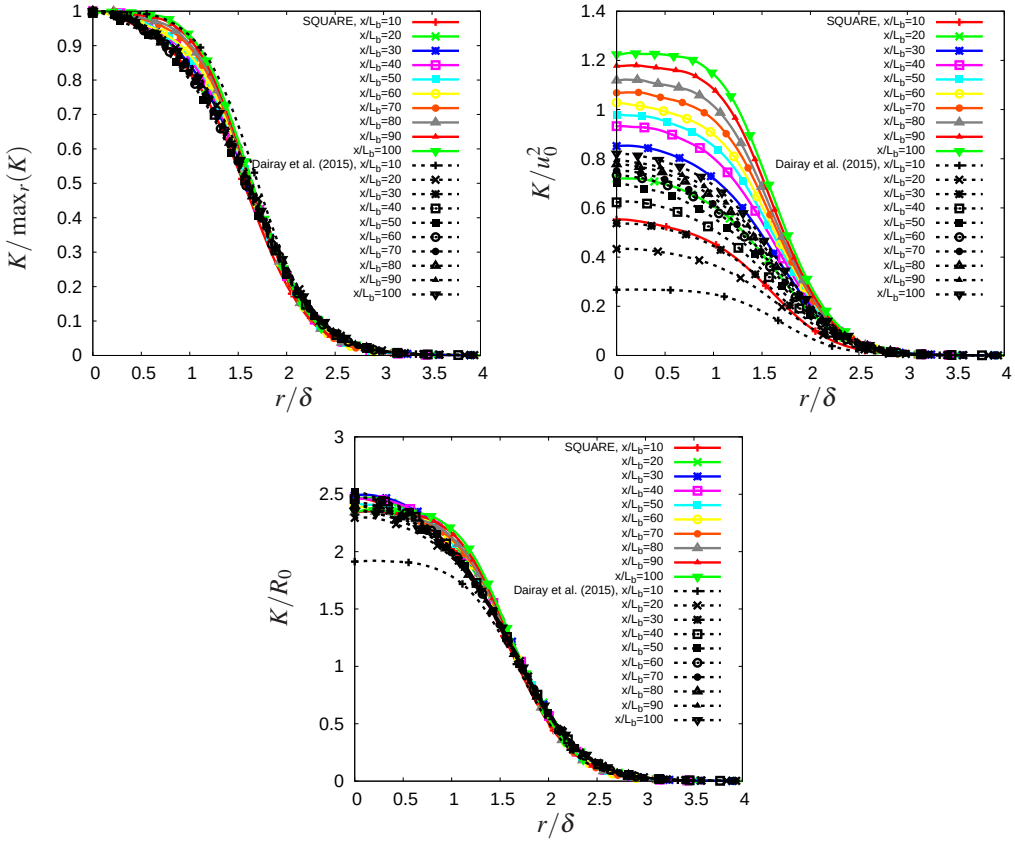

Figure 8: Turbulent kinetic energy profiles at different streamwise distances plotted using similarity scalings with $K_0 = \max_r(K)$ (top left), $K_0 \sim u_0^2$ (top right) and $K_0 \sim R_0 \sim u_0 U_\infty (d\delta/dx)$ (bottom centre) for both the square and irregular plate cases.

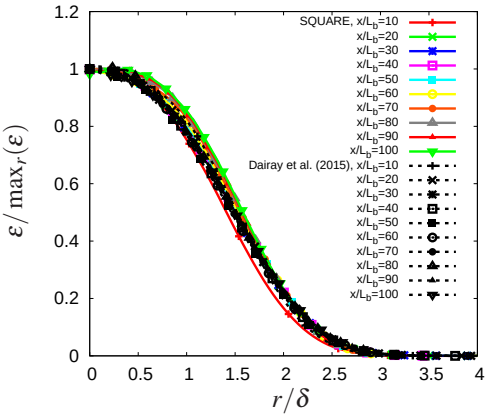

Figure 9: Dissipation profiles at different streamwise distances plotted using similarity scaling with $D_0 = \max_r(\varepsilon)$ for both the square and irregular plate cases.

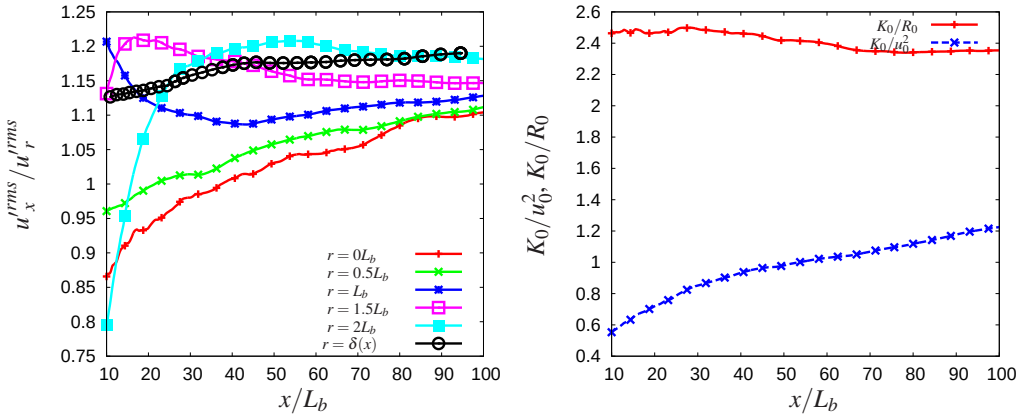

Figure 10: Ratios of the r.m.s. of u_x' to the r.m.s. of u_r' as functions of x/L_b along the centreline ($r = 0$) and on various axisymmetric surfaces $r = L_b/2$, L_b, $3L_b/2$, $2L_b$ and $\delta(x)$ (left) and streamwise evolutions of K_0/u_0^2 and K_0/R_0 (right).

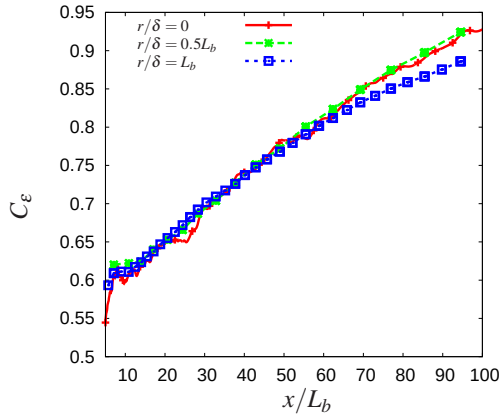

Figure 11: Streamwise variation of the dissipation constant C_ε for the square plate case.

A	α	x_{0A}/θ	B	β	x_{0B}/θ
3.39	-0.89	0.61	0.54	0.45	0.61

Table 1: Best fits to u_0/U_∞ and δ/θ obtained for $x \in [10L_b; 100L_b]$.

irregular plate and also with Obligado et al. (2015) who measured non-constant C_ε in a high Reynolds number turbulent wake generated by a square plate.

To probe the relation between the dissipation law and the scaling laws of u_0 and δ, the DNS data have been fitted with the power laws $u_0(x)/U_\infty = A\left((x-x_{0A})/\theta\right)^\alpha$ and $\delta(x)/\theta = B\left((x-x_{0B})/\theta\right)^\beta$ where x_{0A} and x_{0B} are a priori different virtual origins, but the theory of course requires them to be the same. The fitting method used here is exactly the same as in Dairay et al. (2015) which is an improvement of the original method introduced in Nedić et al. (2013). It returns approximately equal values of the two virtual origins.

The best fit values obtained for $x \in [10L_b; 100L_b]$ are reported in table 1 (see also figure 12). The values of the exponents $\alpha = -0.89$ and $\beta = 0.45$ are found

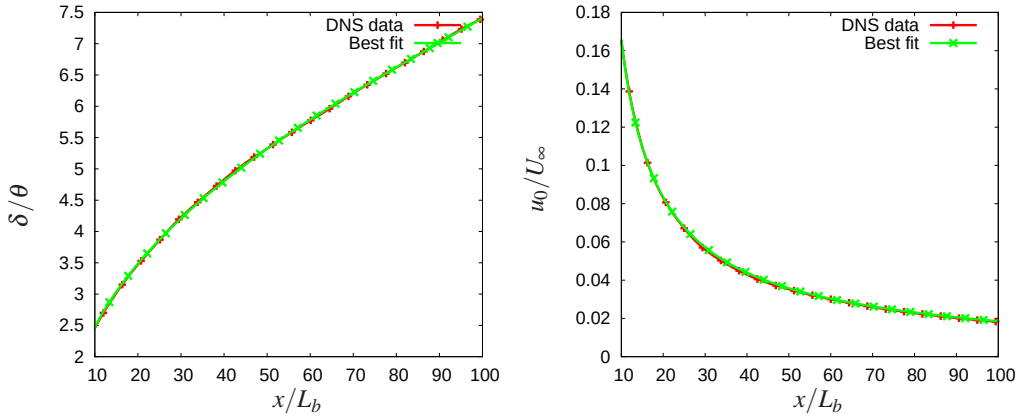

Figure 12: Streamwise evolutions of the integral wake's width (left) and the centreline velocity deficit (right) plotted together with their best fit counterpart.

to be in between the values $\alpha = -2/3$ and $\beta = 1/3$ predicted by the equilibrium theory (corresponding to $m = 0$, *i.e* $C_\varepsilon = const.$, in equation (1)) and the high Reynolds number non-equilibrium exponents $\alpha = -1$ and $\beta = 1/2$ of Nedić et al. (2013); Dairay et al. (2015); Obligado et al. (2015) (corresponding to $m = 1$ in equation (1)). In a recent numerical study, de Stadler et al. (2014) also reported the high Reynolds number non-equilibrium exponents in the wake generated by a sphere. However, as they did not provide information on the turbulence dissipation, the presence of the new dissipation law (1) in their turbulent axisymmetric wakes could not be directly established. As in Dairay et al. (2015), the question arises whether the exponents α and β can be explained by the non-equilibrium predictions stated in section 1. In other words, could the wake laws, observed in the range $x \in [10L_b; 100L_b]$ for the square plate, be also accountable to the dissipation law $C_\varepsilon \sim \left(Re_G^m/Re_l^m\right)$? The value $m \approx 0.7$ returns indeed a very good agreements with our data as illustrated by the constant value of the product $C_\varepsilon \times \left(Re_l^m/Re_G^m\right)$ plotted in figure 13 (left) (see figure11 for compari-

son). In addition, when using non-equilibrium similarity scaling with $m = 0.7$, the dissipation profiles are found to be self-preserving for $x > 20L_b$ as it is illustrated in figure 13 (right). Importantly, this value of m also returns satisfactory agreement with the fitted exponents values when using the theoretical relations $\alpha = -2(1+m)/(3+m)$ and $\beta = (1+m)/(3+m)$ of Dairay et al. (2015). These findings suggest that the wake's width and the velocity deficit scalings are consistent with a non-equilibrium dissipation law that does not exist only in wakes generated by irregular plates but also in more conventionnal axisymmetric and self-preserving wakes (at least for the streamwise extension considered in this study).

Irregular and square plates actually have the same Strouhal number if they are placed normal to the flow and have the same surface area (Nedić et al., 2015). In this respect the large scale structures generated by both plates are not so different. However they do have different energy levels (Nedić et al., 2015). But the main point is that the turbulence has similar if not the same dissipation mechanism in both cases and therefore same dissipation scalings which lead to same wake scalings if the wake is axisymmetric and its U, K, ε and R_{xr} profiles are self-similar. Concerning self-similarity, Johansson et al. (2003) have shown that self-similarity of all terms in the mean momentum and Reynolds stress equations leads to the classical dissipation scaling of Taylor (1935) and Kolmogorov (1941). It is therefore fully consistent with our results that only a few but not all terms of these equations are self-similar.

The non-equilibrium dissipation scaling law in these axisymmetric wakes is also found in other turbulent flows such as turbulence generated by various types of grids (see Vassilicos, 2015) and even Direct Numerical Simulations of both

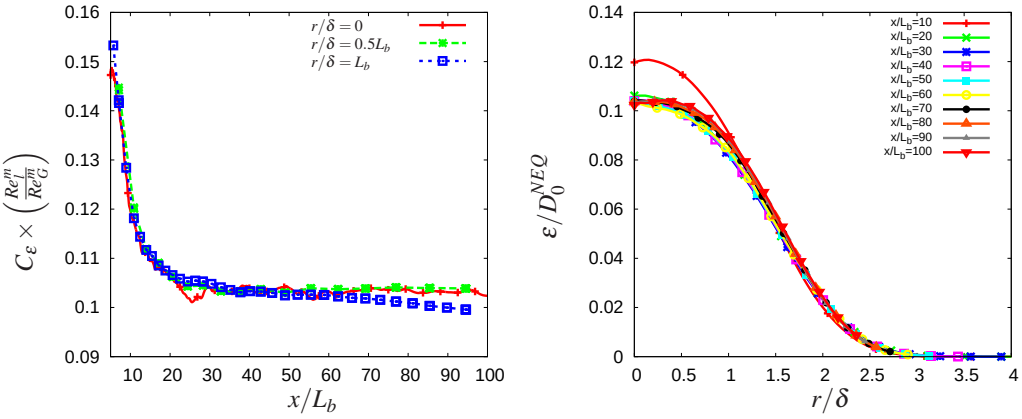

Figure 13: Streamwise variation of the product $C_\varepsilon \times \left(Re_l^m/Re_G^m\right)$ (left) and dissipation profiles at different streamwise distances plotted using non-equilibrium similarity scaling with $D_0^{NEQ} = (U_\infty l/\nu)^m (u_0\delta/\nu)^{-m} K_0^{3/2}/\delta$ for $m = 0.7$.

decaying and forced periodic turbulence (see Goto and Vassilicos, 2015). We are therefore not dealing with an uninteresting initial transient but with a non-equilibrium behaviour which characterises some universality class of turbulent flows.

6. Conclusion

DNS of a spatially developing turbulent wake generated by a square plate shows that (i) the profiles of U, R_{xr}, K and ε are self-similar for $x \geq 20L_b$; (ii) the turbulent kinetic energy and the Reynolds shear stress scale together and do not scale as u_0^2, in agreement with an assumption of constant anisotropy introduced in Dairay et al. (2015); (iii) for the streamwise extension considered in this study, the wake width and velocity deficit scalings are in agreement with the non-equilibrium dissipation law (1), where the exponent m may depend on distance from and/or geometry of the wake generator.

Acknowledgements

The authors were supported by an ERC Advanced grant (2013-2018) awarded to J.C. Vassilicos. The simulations were performed at the PDC Centre for High Performance Computing at the KTH Royal Institute of Technology (Sweden) with resources provided by the DECI-11 project FRAPLAWI (EC funding RI-312763). The authors acknowledge the UK Turbulence Consortium (EPSRC research grant no. EP/L000261/1) for access to UK supercomputing resources. The authors also thank PRACE for awarding access to the SuperMUC supercomputer based at Leibniz-Rechenzentrum (Leibniz Supercomputing Centre) in Germany.

References

Dairay, T., Obligado, M., Vassilicos, J.C., 2015. Non-equilibrium scaling laws in axisymmetric turbulent wakes. J. Fluid Mech 781, 166–195.

George, W.K., 1989. The self-preservation of turbulent flows and its relation to initial conditions and coherent structures, in: George, W.K., Arndt, R. (Eds.), Advances in Turbulence. Springer, pp. 39–73.

Goto, S., Vassilicos, J., 2015. Energy dissipation and flux laws for unsteady turbulence. Physics Letters A 379, 1144–1148.

Johansson, P.B.V., George, W.K., Gourlay, M.J., 2003. Equilibrium similarity, effects of initial conditions and local Reynolds number on the axisymmetric wake. Phys. Fluids 15, 603–617.

Kolmogorov, A.N., 1941. Dissipation of energy in locally isotropic turbulence, in: Akademiia Nauk SSSR Doklady, p. 16.

Laizet, S., Lamballais, E., 2009. High-order compact schemes for incompressible flows: a simple and efficient method with quasi-spectral accuracy. J. Comp. Phys. 228, 5989–6015.

Laizet, S., Lamballais, E., Vassilicos, J.C., 2010. A numerical strategy to combine high-order schemes, complex geometry and parallel computing for high resolution DNS of fractal generated turbulence. Computers and Fluids 39, 471–484.

Laizet, S., Li, N., 2011. Incompact3d: a powerful tool to tackle turbulence problems with up to $O(10^5)$ computational cores. Int. J. Numer. Methods Fluids 67, 1735–1757.

Laizet, S., Nedić, J., Vassilicos, J.C., 2015. Influence of the spatial resolution on fine-scale features in DNS of turbulence generated by a single square grid. Int. J. of Computational Fluid Dynamics 29, 286–302.

Lamballais, E., Fortuné, V., Laizet, S., 2011. Straightforward high-order numerical dissipation via the viscous term for direct and large eddy simulation. J. Comp. Phys. 230, 3270–3275.

Lele, S.K., 1992. Compact finite difference schemes with spectral-like resolution. J. Comp. Phys. 103, 16–42.

Nedić, J., Supponen, O., Ganapathisubramani, B., Vassilicos, J., 2015. Geometrical influence on vortex shedding in turbulent axisymmetric wakes. Physics of Fluids (1994-present) 27, 035103.

Nedić, J., Vassilicos, J.C., Ganapathisubramani, B., 2013. Axisymmetric turbulent wakes with new nonequilibrium similarity scalings. Physical review letters 111, 144503.

Obligado, M., Dairay, T., Vassilicos, J.C., 2015. Non-equilibrium scalings of turbulent wakes. Submitted to Physical review letters .

Pantano, C., Sarkar, S., 2002. A study of compressibility effects in the high-speed turbulent shear layer using direct simulation. Journal of Fluid Mechanics 451, 329–371.

Parnaudeau, P., Carlier, J., Heitz, D., Lamballais, E., 2008. Experimental and numerical studies of the flow over a circular cylinder at Reynolds number 3900. Phys. Fluids 20, 085101.

Redford, J.A., Castro, I.P., Coleman, G.N., 2012. On the universality of turbulent axisymmetric wakes. J. Fluid Mech. 710, 419–452.

de Stadler, M., Rapaka, N., Sarkar, S., 2014. Large eddy simulation of the near to intermediate wake of a heated sphere at Re= 10,000. International Journal of Heat and Fluid Flow 49, 2–10.

Taylor, G.I., 1935. Statistical theory of turbulence, in: Proceedings of the Royal Society of London A: Mathematical, Physical and Engineering Sciences, The Royal Society. pp. 421–444.

Townsend, A.A., 1976. The structure of turbulent shear flow. Cambridge university press.

Vassilicos, J.C., 2015. Dissipation in turbulent flows. Ann. Rev. Fluid Mech. 47, 95–114.